

Vibe Nylander,<sup>1</sup> Lars R. Ingerslev,<sup>1</sup> Emil Andersen,<sup>1</sup> Odile Fabre,<sup>1</sup> Christian Garde,<sup>1</sup> Morten Rasmussen,<sup>1</sup> Kiymet Citirikkaya,<sup>1</sup> Josephine Bæk,<sup>1</sup> Gitte L. Christensen,<sup>2</sup> Marianne Aznar,<sup>3</sup> Lena Specht,<sup>3,4</sup> David Simar,<sup>5</sup> and Romain Barrès<sup>1</sup>



# Ionizing Radiation Potentiates High-Fat Diet–Induced Insulin Resistance and Reprograms Skeletal Muscle and Adipose Progenitor Cells

Diabetes 2016;65:3573–3584 | DOI: 10.2337/db16-0364

**Exposure to ionizing radiation increases the risk of chronic metabolic disorders such as insulin resistance and type 2 diabetes later in life. We hypothesized that irradiation reprograms the epigenome of metabolic progenitor cells, which could account for impaired metabolism after cancer treatment. C57Bl/6 mice were treated with a single dose of irradiation and subjected to high-fat diet (HFD). RNA sequencing and reduced representation bisulfite sequencing were used to create transcriptomic and epigenomic profiles of preadipocytes and skeletal muscle satellite cells collected from irradiated mice. Mice subjected to total body irradiation showed alterations in glucose metabolism and, when challenged with HFD, marked hyperinsulinemia. Insulin signaling was chronically disrupted in skeletal muscle and adipose progenitor cells collected from irradiated mice and differentiated in culture. Epigenomic profiling of skeletal muscle and adipose progenitor cells from irradiated animals revealed substantial DNA methylation changes, notably for genes regulating the cell cycle, glucose/lipid metabolism, and expression of epigenetic modifiers. Our results show that total body irradiation alters intracellular signaling and epigenetic pathways regulating cell proliferation and differentiation of skeletal muscle and adipose progenitor cells and provide a possible mechanism by which irradiation used in cancer treatment increases the risk for metabolic disease later in life.**

Exposure to ionizing radiation increases the risk of developing chronic diseases such as cancer or cardiovascular

diseases (1,2). Patients with cancer treated with radiation therapy have increased risk for developing metabolic disorders such as type 2 diabetes, hyperinsulinemia, and components of the metabolic syndrome (3–6). Yet, the molecular mechanisms responsible for metabolic dysfunction after irradiation remain unknown.

Ionizing radiation generates free radicals in exposed cells and tissues, resulting in DNA damage, to which highly proliferative cells, like cancer cells, are most susceptible (7). Progenitor cells, including skeletal muscle satellite cells, are more sensitive to ionizing radiation than their differentiated counterparts (8). Given the predominant role of skeletal muscle and adipose tissue in the regulation of whole-body glucose and lipid metabolism (9,10), ionizing radiation could reprogram skeletal muscle and adipose progenitor cells, leading to altered differentiation and subsequent alterations in cell function and whole-body glucose homeostasis.

Epigenetic factors that have the potential to be inherited along cell division may mediate long-term effects on gene expression. DNA methylation is a major epigenetic factor programming cell fate and differentiation through the regulation of cell type-specific gene expression programs (11). Numerous studies have provided evidence that ionizing radiation can influence DNA methylation by decreasing DNA methyl transferase (DNMT) expression or alternatively through the production of molecules derived from reactive oxygen species (12–15). Given that muscle satellite cells contribute to regeneration of muscle

<sup>1</sup>Faculty of Health and Medical Sciences, Novo Nordisk Foundation Center for Basic Metabolic Research, University of Copenhagen, Copenhagen, Denmark

<sup>2</sup>Department of Biomedical Sciences, University of Copenhagen, Copenhagen, Denmark

<sup>3</sup>Department of Oncology, Section of Radiotherapy, Rigshospitalet, University of Copenhagen, Copenhagen, Denmark

<sup>4</sup>Department of Hematology, Rigshospitalet, University of Copenhagen, Copenhagen, Denmark

<sup>5</sup>Inflammation and Infection Research, School of Medical Sciences, University of New South Wales, Sydney, Australia

Corresponding author: Romain Barrès, barres@sund.ku.dk.

Received 21 March 2016 and accepted 14 September 2016.

This article contains Supplementary Data online at <http://diabetes.diabetesjournals.org/lookup/suppl/doi:10.2337/db16-0364/-/DC1>.

D.S. and R.B. are shared last authors.

© 2016 by the American Diabetes Association. Readers may use this article as long as the work is properly cited, the use is educational and not for profit, and the work is not altered. More information is available at <http://www.diabetesjournals.org/content/license>.

under various stressors like exercise or muscle damage (16–19), modulation of DNA methylation in satellite cells may alter long-term muscle function. In this study, we tested the hypothesis that ionizing radiation induces chronic alteration of the epigenome of skeletal muscle and adipose progenitor cells. We determined whether ionizing radiation alters whole-body glucose homeostasis and reprograms metabolic progenitor cells.

## RESEARCH DESIGN AND METHODS

### Animals

Experiments were approved by the Danish Animal Experiments Inspectorate and performed according to the local committee guidelines. Male C57Bl/6 mice (Taconic Farms) were housed at standard 12:12 light/dark cycle; food and water were available *ad libitum*. Mice were euthanized by cervical dislocation.

Ten-week-old mice were irradiated with a single dose of 6 Gy ( $^{137}\text{Cs}$  source) ( $N = 30$ ) in a Gammacell 40 Exactor (Best Theratronics). Nonirradiated mice ( $N = 30$ ) were sham treated. Mice received a standard chow diet (chow; Research Diets) for the first 6 weeks and then either chow or high-fat diet (HFD) containing 60% energy intake from fat (Research Diets) for the remainder of the experiment. After 14 weeks of HFD, half of the cohort was euthanized, and satellite cells were isolated ( $N = 6$ ); the remaining mice were fed either chow or HFD for 20 weeks (total of 34 weeks), after which preadipocytes and pancreatic islets were isolated ( $N = 6$ ).

For studying the acute effects of irradiation, animals received a single dose of 3 or 6 Gy ( $^{137}\text{Cs}$  source) in a Gammacell 40 Exactor (Best Theratronics).

Metabolic characterization is detailed in the Supplementary Data.

### Muscle Satellite Cells, Pancreatic Islets, and Preadipocyte Isolation and Culture

Isolation of satellite cells ( $N = 6$ ) was performed as described (19) and further detailed in the Supplementary Data. Epididymal adipose tissue was collected from mice ( $N = 6$ ). The stromal vascular fraction (SVF) was isolated by digestion with Collagenase I (Life Technologies). Cells were cultured in DMEM 25 mmol/L glucose (Life Technologies) with 10% FBS (Sigma-Aldrich) and 1% penicillin/streptomycin (P/S; Life Technologies) mix while proliferating. Differentiation was initiated in confluent cultures by addition of 5  $\mu\text{g/mL}$  insulin, 0.5 mmol/L isobutylmethylxanthine, 1 mmol/L dexamethasone, and 10  $\mu\text{mol/L}$  rosiglitazone. Pancreatic islet isolation ( $N = 6$ ) was performed as previously described (20).

### Immunoblotting

Differentiated primary cells and L6 cells were serum deprived for 4 h or overnight, respectively, before stimulation with 15 or 100 nmol/L insulin for 5 min. Proteins were solubilized in 20 mmol/L Tris, 150 mmol/L NaCl, 5 mmol/L EDTA, 150 mmol/L NaF, 2 mmol/L  $\text{Na}_3\text{VO}_4$ , 10 mmol/L Na-pyrophosphate, 0.5 mmol/L phenylmethylsulfonyl

fluoride, and 1% Triton X-100. For nuclear protein extracts, gastrocnemius skeletal muscle was dissected 24 h postirradiation and snap-frozen, or irradiated L6 cells were lysed 24 h postirradiation. Tissue or cells were homogenized in hypotonic buffer containing protease and phosphatase inhibitors (Active Motif), and nuclear extraction was performed according to manufacturer protocol (Active Motif).

Protein concentration was measured by bicinchoninic acid assay (Pierce BCA Protein Assay Kit; Thermo Fisher Scientific). Protein samples were resolved by SDS-PAGE on a Mini-PROTEAN tetra cell system (Bio-Rad) and transferred into a polyvinylidene difluoride membrane (Millipore) using an ECL semidry transfer unit (Amersham Biosciences). Polyvinylidene difluoride membranes were blocked in 2% skimmed milk in Tris-buffered saline with Tween-20 (0.1% Tween) for 1 h, washed in Tris-buffered saline with Tween-20, and incubated with the respective primary antibody (Ab) overnight at 4°C. After incubation with secondary Ab for 1 h, proteins were detected using the ImmunoStar WesternC Chemiluminescence kit (Bio-Rad). Images acquisition was done with a Molecular Imager ChemiDoc XRS+ (Bio-Rad), and images were analyzed using ImageLab software (Bio-Rad). Primary and secondary Abs were: phospho-extracellular signal-regulated kinase (ERK; Thr<sup>202</sup>/Tyr<sup>204</sup>), ERK, phospho-AKT (Thr<sup>308</sup>), AKT, GAPDH, phospho-IGF receptor (IGFR; Tyr<sup>1135/1136</sup>)/insulin receptor (IR; Tyr<sup>1150/1151</sup>), IR $\beta$ ,  $\beta$ -actin,  $\beta$ -tubulin, Lamin A/C (all from Cell Signaling Technology), DNMT1, DNMT3A, DNMT3B (Abcam), goat anti-rabbit IgG horseradish peroxidase conjugate, and goat anti-mouse IgG horseradish peroxidase conjugate (Bio-Rad).

### DNA Methylation Analysis

Reduced representation bisulfite sequencing (RRBS) and methylated DNA capture sequencing were performed as described (21,22) on satellite cells ( $N = 6$ ). RRBS was performed on SVF cultures ( $N = 6$ ). Methods are detailed in the Supplementary Data.

### RNA Sequencing

Total RNAs ( $N = 6$ ) were isolated with TRIzol reagent (Life Technologies) or a Allprep DNA/RNA/miRNA Universal Kit (Qiagen) according to the manufacturer's protocols. RNA sequencing was performed according to Illumina TruSeq Stranded Total RNA with Ribo-Zero Gold protocol (Illumina). Total RNAs were depleted for ribosomal RNA, fragmented, and cDNA was synthesized using SuperScript III Reverse Transcriptase (Thermo Fisher Scientific). cDNA was subjected to a cleanup using AMPure beads (Beckman Coulter) and adenylated to prime for adapter ligation. After a cleanup using AMPure beads, DNA fragments were amplified using PCR with the following settings: 30 s, 98°C; (10 s, 98°C; 30 s, 60°C; 30 s, 72°C)  $\times$  9–13 cycles; 5 min, 72°C, followed by a final cleanup. The cycle number (9 to 13) was set to prevent saturation and overamplification of individual samples. Libraries were quality-controlled using a Bioanalyzer instrument (Agilent Technologies) and subjected

to 100-bp single-end sequencing on HiSeq 2500 (Illumina) at the Danish National High-Throughput DNA Sequencing Centre. A total of 756.8 million reads was generated. On average, 24.4 million reads/sample were assigned to a gene, and 12,364 genes survived the expression cutoff.

### L6 Cell Line Cultures

L6 cells were grown in minimum essential medium  $\alpha$  with 10% FBS and 1% P/S. Differentiation was induced in minimum essential medium  $\alpha$ , 2% FBS, and 1% P/S. Cells were irradiated with 1, 2, 3, or 6 Gy using an X-ray linear accelerator (Varian Medical Systems), energy  $\sim 2$  MeV, and dose rate of 1 Gy/min ( $N = 3$ ). Cells recovered from irradiation for 3 (2 Gy) or 4 weeks (1, 3, and 6 Gy) while being maintained in the proliferative, nonconfluent phase. Two Gy irradiated cells was treated or not with 100  $\mu\text{g/mL}$  vitamin C, 5  $\mu\text{mol/L}$  vitamin E, or 500  $\mu\text{mol/L}$  folate in combination with 50  $\mu\text{mol/L}$  vitamin B12. These treatments were added 1 h prior to irradiation and continued until 2 days postirradiation.

### DNMT Activity Assay, Reactive Oxygen Species Measurement, and Proliferation Assay

See Supplementary Data.

### Quantitative RT-PCR

Quantitative RT-PCR (qRT-PCR) was performed on selected genes using conventional methodology (21) and is further detailed in the Supplementary Data. Primer sequences are detailed in Supplementary Table 8.

### Accession Numbers

Sequencing data have been archived in a publicly accessible database at the Gene Expression Omnibus (<http://www.ncbi.nlm.nih.gov/geo>) under accession number GSE86280.

### Bioinformatics

For methylated DNA capture sequencing, reads were preprocessed with trimmomatic (23) using the parameters LEADING:3 TRAILING:3 SLIDINGWINDOW:4:15 MINLEN:15 and trimmed for Illumina primers. The preprocessed reads were aligned to the mm10 genome using bowtie2 (24) with the very-sensitive setting. Picard-tools markDuplicates were used to remove duplicates. The read coverage of CpG islands, CpG shores, RefSeq promoters defined as  $\pm 1,000$  bp from transcription start site, and RefSeq exons were computed with featureCounts (25), extending reads to 253 bp; the median length was estimated by Bioanalyzer (Agilent Technologies). Regions surviving a 1-read/kb of transcript per million mapped reads in  $>12$  samples inclusion criterion were tested for differential methylation with edgeR (26) using the glmFit/glmLRT functions and tagwise dispersion.

For RRBS, reads were preprocessed with Trim Galore v0.4.0 and Cutadapt v1.8.3 using standard settings and the `-rrbs` flag. Preprocessed reads were aligned to the mm10 genome and CpG coverage computed using bismark v0.14.4 (27) assisted by bowtie2 v2.2.6 (24).

Methylation levels were estimated using BiSeq v1.10 (28). Settings were as in the manual, except for the function:

“clusterSites”, which was run with the parameters `perc.samples = 3/6` and `min.sites = 5`. A custom model fitting script was used to allow for multivariate modeling. The model used was `formula = ~Radiation*Diet | Radiation + Diet`. Final trimmed clusters were detected with a false discovery rate (FDR) cutoff of 0.1. Differences in methylation are given as “median methylation for nonirradiated control–median methylation for irradiated samples.” Therefore, negative values of methylation correspond to higher methylation in irradiated samples. Analysis of gene ontology was performed using Gprofiler, and clustering of gene ontology terms was performed in Revigo.

For RNA sequencing, reads were preprocessed with Trim galore v0.4.0 on default settings and mapped to the mm10 genome using tophat2 (29) with the `-very-sensitive` setting. The exonic read coverage was computed with featureCounts (30), with an inclusion criterion of 1 count/min in more than six samples, and tests for differential gene expression were conducted using edgeR (26) followed by correction for multiple testing with the Benjamini-Hochberg method. Gene ontology analysis was performed to determine functional classification of genes differentially expressed between irradiated and nonirradiated cells using DAVID (31) and GOrilla softwares (32).

### Statistics

Statistical analysis was performed using SigmaPlot (Systat Software) or SPSS (SPSS Inc.). Normality was tested using the skewness and kurtosis tests. Statistical difference between two groups was analyzed by Student *t* test. Differences in weight and magnetic resonance imaging data, as well as Western blot and qRT-PCR analyses, were analyzed by two-way ANOVA, with Tukey multiple-corrections test. Analysis of indirect calorimetry data was performed with 12-h intervals using repeated-measures ANOVA. A *P* value  $\leq 0.05$  was considered statistically significant.

## RESULTS

### Irradiation Predisposes to Metabolic Dysfunction Under Nutritional Stress

To investigate the long-term effects of ionizing radiation on glucose metabolism, adult mice were subjected to a single, nonlethal dose (6 Gy) of  $\gamma$ -radiation. Prior to irradiation and the first 6 weeks after irradiation, mice received a chow diet. In response to irradiation, mice exhibited decreased body weight despite preserved food intake and energy expenditure (Fig. 1A and Supplementary Fig. 1A and B). Changes in both fat and lean mass accounted for the difference in body weight, which was conserved throughout the life of the animals (Supplementary Fig. 1C). At 12 weeks postirradiation, irradiated mice were more glucose tolerant compared with control-treated mice (Fig. 1B), whereas glucose tolerance was similar between groups 25 weeks after irradiation (corresponding to 19 weeks of HFD) (Fig. 1C). Insulin resistance at 34 weeks after irradiation, as assessed by the HOMA of insulin resistance index, tended to be lower in irradiated animals

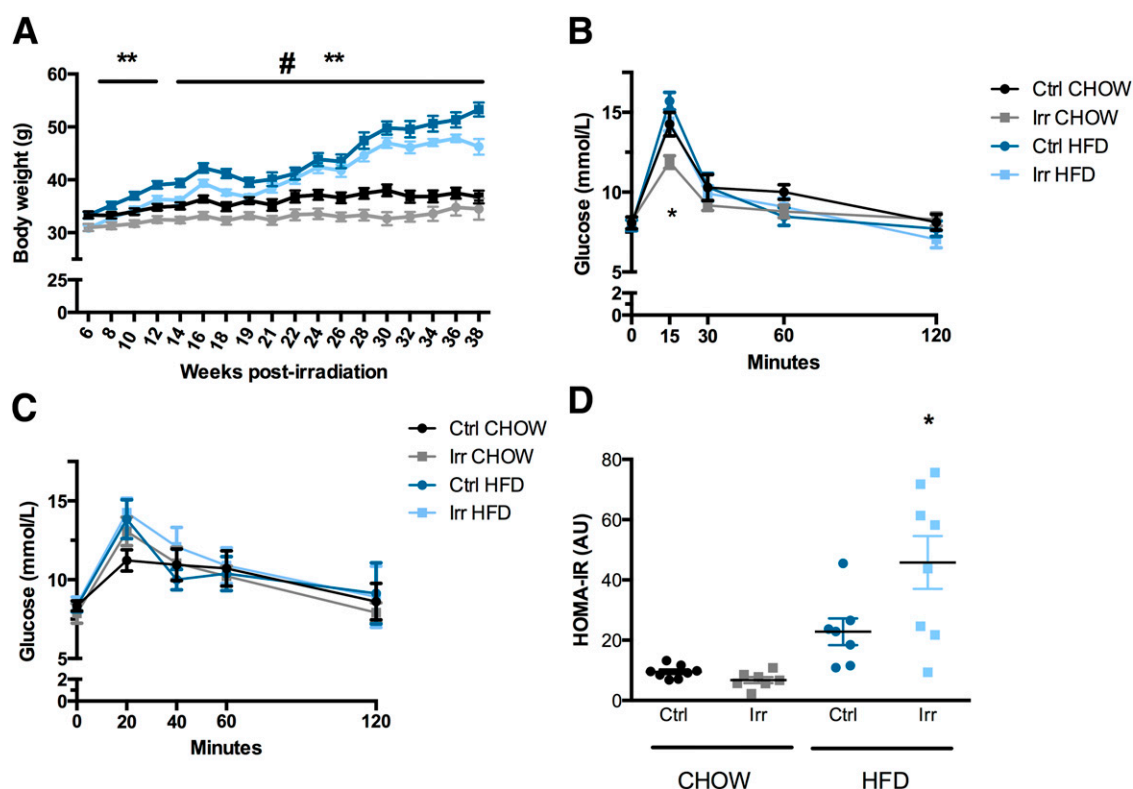


**Figure 1**—Irradiation alters body weight and whole-body metabolism. Ten-week-old C57Bl/6 mice were irradiated or sham treated. **A:** Body weight throughout the study ( $N = 7$ – $15$ ). Oral glucose tolerance was tested 6 weeks into HFD (11 weeks postirradiation;  $N = 11$ – $15$ ) (**B**) and 19 weeks into HFD ( $N = 7$  to  $8$ ) (**C**). **D:** HOMA index of insulin resistance (HOMA-IR) was calculated 28 weeks into HFD ( $N = 7$  to  $8$ ). Error bars are SEM. \* $P < 0.05$ , \*\* $P < 0.05$  for irradiation only; # $P < 0.05$  for HFD only. AU, arbitrary units; Ctrl, nonirradiated; Irr, irradiated.

fed a chow diet, although this difference did not reach statistical significance (Fig. 1D). Fasting plasma glucose was unchanged after irradiation (Supplementary Fig. 1D).

To determine the metabolic response under nutritional stress, irradiated mice were subjected to HFD (60%) from 6 weeks postirradiation. As expected, adiposity was higher in animals under an HFD (Supplementary Fig. 1C). Irradiation lowered the effect of HFD (Supplementary Fig. 1C). Insulin resistance was higher in mice subjected to irradiation and HFD (Fig. 1D). In pancreatic islets isolated 40 weeks after irradiation, expression of the insulin or glucagon genes was unaltered in irradiated mice fed an HFD (Supplementary Fig. 1E and F). Collectively, these results show that irradiation affects both fat and lean mass and has deleterious effects on insulin sensitivity when animals are subjected to nutritional stress.

### Ionizing Radiation Impairs Preadipocyte Differentiation and Function

To investigate whether irradiation specifically alters adipose tissue, the adipogenic potential of preadipocytes from irradiated animals was determined. Cultures from the SVF collected from mice 40 weeks after irradiation (6 Gy) were established, and differentiation was quantified using expression analysis of adipogenic genes. SVF cultures from irradiated mice showed lower adipogenic potential as

evidenced by lower expression of the adipokine adiponectin (*Adipoq*) (Fig. 2A). Expression of the master adipogenic factor peroxisome proliferator-activated receptor  $\gamma$  tended to be lower in irradiated mice compared with controls, although this did not reach statistical significance (Fig. 2A). Moreover, protein levels of IR $\beta$ /IGFR were markedly lower in SVF cultures isolated from irradiated mice (Fig. 3A). Altogether, these data suggest a reduced adipogenic potential in irradiated animals. Although expression of the cyclin-dependent kinase inhibitor (*Cdkn*)-1c was similar between groups (Fig. 2B), *Cdkn2a* expression was lower in proliferating cells, whereas *Cdkn2a* and *p19* expression was higher in differentiated cells from irradiated mice (Fig. 2C). Thus, ionizing radiation not only impairs adipogenic potential, but also regulation of the cell cycle. Macrophage infiltration can contribute to development of glucose intolerance and insulin resistance (33,34). Expression of the macrophage marker *F4/80* was similar in all cultures, indicating that macrophage infiltration does not contribute to alteration in adipose tissue function of irradiated mice (Fig. 2A). The insulin-signaling pathway was studied to further characterize metabolic features of isolated progenitor cells. Basal phosphorylation of IR $\beta$ /IGFR, ERK, and AKT were higher in irradiated mice (Fig. 3B and C). Strikingly, upon insulin stimulation, phosphorylation of IR $\beta$ /IGFR and AKT was not as elevated as in control mice

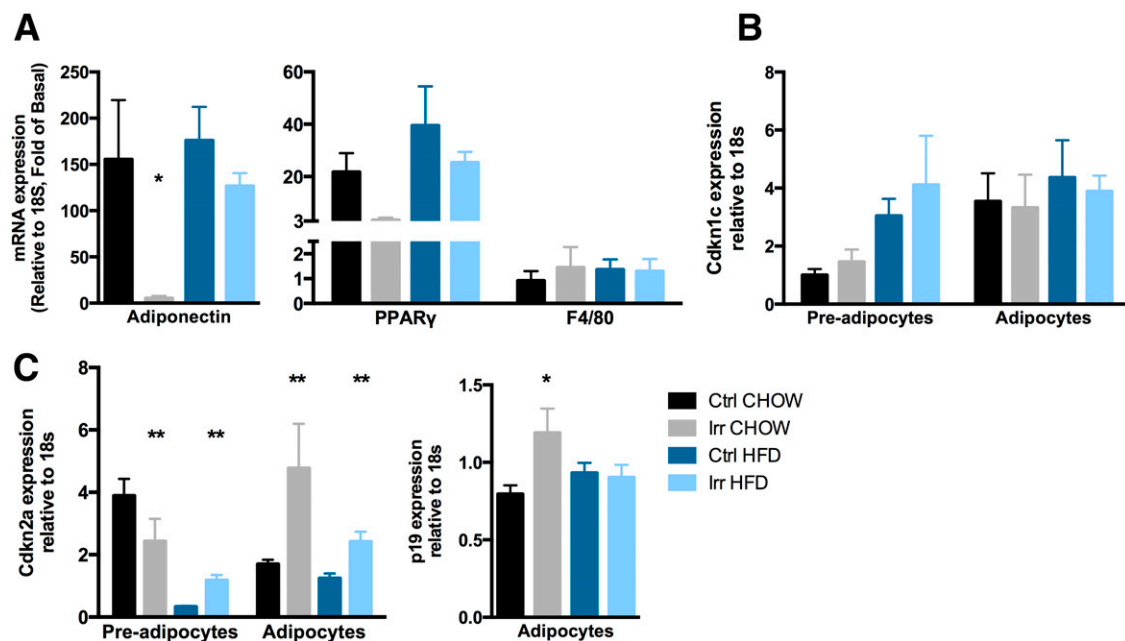


**Figure 2**—Irradiation decreases adipogenic potential of preadipocytes. Cells from the SVF were isolated from irradiated (6 Gy) and non-irradiated mice and cultured for 1–3 weeks before differentiation was induced. **A:** Gene expression of adipogenic and macrophage genes was determined on differentiated cells by qRT-PCR ( $N = 3$ –7). **B and C:** Gene expression of senescence markers was determined by RT-qPCR ( $N = 3$ –7). Error bars are SEM. \* $P < 0.05$ , \*\* $P < 0.05$  for irradiation only. Ctrl, nonirradiated; Irr, irradiated; PPAR $\gamma$ , peroxisome proliferator-activated receptor  $\gamma$ .

(Fig. 3D and E), whereas ERK phosphorylation was unchanged (Fig. 3F). These results suggest that the metabolic action of insulin is altered in adipocytes from irradiated mice. Collectively, these results show that preadipocytes carry a persistent memory of ionizing radiation and suggest that ionizing radiation causes dysfunctional preadipocyte proliferation and differentiation.

To investigate whether such memory of ionizing radiation is mediated by changes in epigenetic modifications, genome-wide DNA methylation profile of preadipocytes exposed to ionizing radiation was determined. RRBS showed that irradiated cells have a marked alteration of the DNA methylation profile, with 3,241 differentially methylated genes ( $P < 0.05$ ; FDR  $< 0.1$ ) compared with nonirradiated control cells (Supplementary Table 1). Gene ontology analysis identified significant enrichment of pathways related to regulation of primary metabolic process, chromatin modification, and cellular response to stress, as well as pathways involved in regulation of developmental and cell cycle processes (Supplementary Fig. 2B). Taken together, these results indicate that ionizing radiation reprograms the preadipocytes and suggest a contribution of epigenetic factors in altered proliferation and differentiation of the adipocyte lineage.

#### **Ionizing Radiation Alters Proliferation and ERK Signaling of Muscle Progenitor Cells**

The effect of irradiation on lean mass prompted us to investigate the effect of ionizing radiation on cell proliferation and insulin signaling in skeletal muscle progenitor cells. The proliferation rate of satellite cells isolated 20 weeks

postirradiation (6 Gy) was 30% lower than nonirradiated cells (Fig. 4A). Insulin-stimulated AKT phosphorylation was similar, whereas ERK phosphorylation was increased twofold higher collected from irradiated mice and differentiated into myotubes (Fig. 4B–D). Given that the balance between AKT and ERK signaling has been implicated in insulin resistance (35), our results suggest that reprogramming of insulin action in the differentiated muscle cell by ionizing radiation may affect cell proliferation and metabolism.

#### **Ionizing Radiation Remodels DNA Methylation of Muscle Progenitor Cells**

To determine whether ionizing radiation also reprograms muscle progenitor cells through epigenetic processes, genome-wide DNA methylation analysis was performed on skeletal muscle progenitor cells isolated from mice 20 weeks postirradiation. Using methylated DNA capture sequencing, we found 3,104 differentially methylated regions (DMRs) between irradiated and nonirradiated mice, 84 DMRs within CpG islands, and 373 DMRs within promoter regions ( $P < 0.05$ ; FDR  $< 0.1$ ) (Supplementary Table 2). The remaining DMRs were located in intragenic regions. Within the list, several genes of interest were highlighted because of their role in epigenetic processes or regulation of cell cycle and metabolism.

Analysis by qRT-PCR for the selected genes of interest showed an inverse association between DNA methylation and gene expression for the eukaryotic initiation factor 2b isoform 1 (*eIF2b*) (Fig. 5A and Supplementary Table 2),



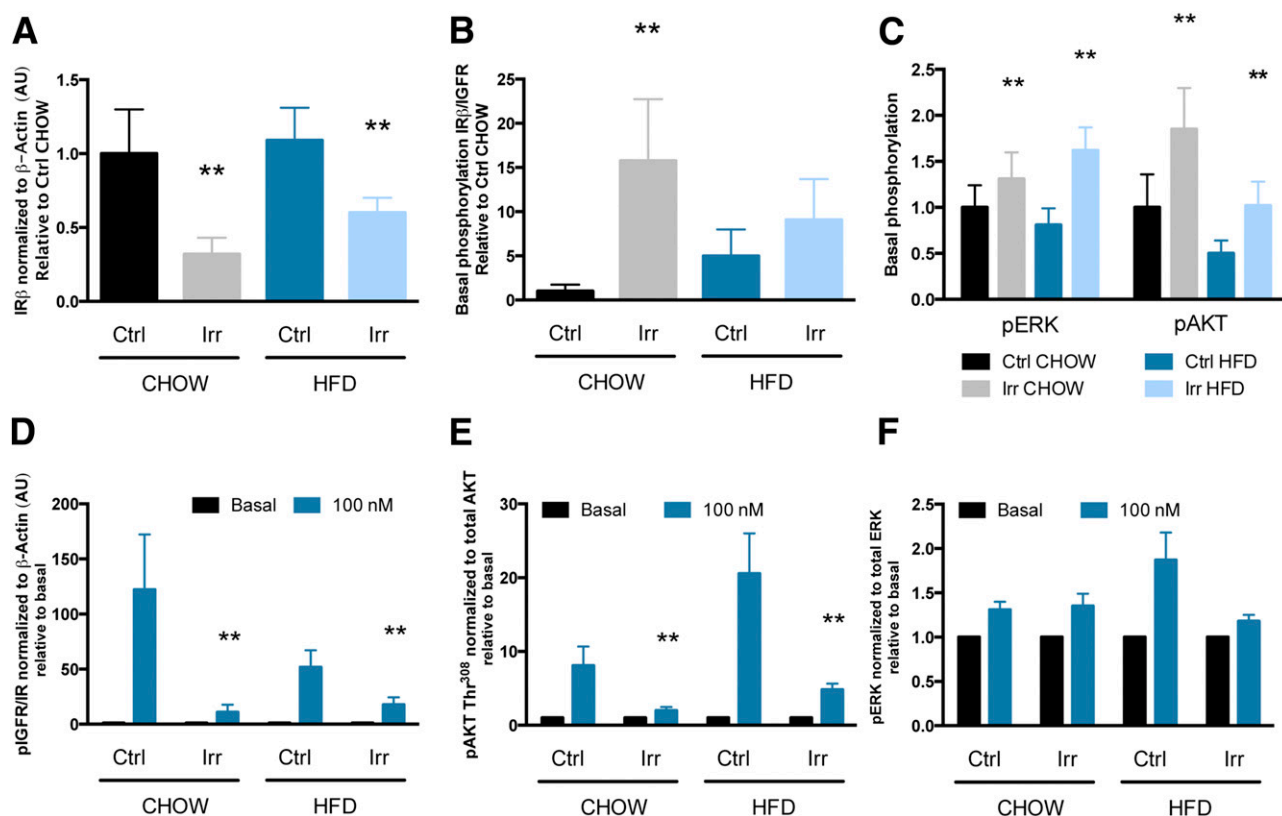


**Figure 3**—Insulin signaling is decreased in irradiated preadipocytes. Cells from the SVF were isolated from irradiated (6 Gy) and non-irradiated mice and cultured for 1–3 weeks before differentiation was induced ( $N = 6$ ). On day 8 of differentiation, cells were stimulated with 0 or 100 nmol/L insulin for 5 min ( $N = 5$ –7). **A**: Quantification of IR expression relative to actin. Data are represented relative to Ctrl chow. **B**: Quantification of IR $\beta$ /IGFR basal phosphorylation normalized to  $\beta$ -actin levels and shown relative to Ctrl chow. **C**: Basal phosphorylation of ERK and AKT is normalized to total ERK and AKT levels, respectively, and shown relative to Ctrl chow. **D**: Insulin-stimulated phosphorylation of IGFR/IR is normalized to  $\beta$ -actin levels and shown relative to basal phosphorylation of Ctrl chow. Insulin-stimulated phosphorylation of AKT (**E**) and ERK (**F**). Data are presented as fold of basal phosphorylation. Error bars are SEM. \*\* $P < 0.05$  for irradiation only. AU, arbitrary units; Ctrl, nonirradiated; Irr, irradiated.

whereas DNA methyl transferase 1 (*Dnmt1*) and *Cdkn1c* showed either no or a positive association, respectively (Fig. 5B and C and Supplementary Table 2). Expression, but not methylation, of *Cdkn2a*, another master cell-cycle regulator, was fivefold lower in cells from irradiated mice (Fig. 5D). Gene expression of the remaining genes of interest was similar among all groups (Supplementary Fig. 3A–C). To obtain better resolution at the specific differentially methylated cytosines, DNA methylation was analyzed by RRBS. We found 9,827 regions to be differentially methylated between cells isolated from irradiated and nonirradiated mice. The differentially methylated cytosines occurred in 4,583 genes ( $P < 0.05$ ; FDR  $< 0.1$ ) (Supplementary Table 3). Similarly to adipocytes, DMRs were found at proximity of genes involved in metabolic process, cellular response to DNA damage, and cell proliferation (Supplementary Fig. 3D). To investigate the mechanism by which irradiation alters DNA methylation in skeletal muscle, we measured DNMT activity 24 h postirradiation in skeletal muscle from irradiated mice and in L6 myocyte cultures. Although total DNMT activity was not changed in muscle or cells (Fig. 6A and B), the fact that nuclear

expression of DNMT1 (but not DNMT3A or DNMT3B) was lower in muscle from irradiated animals (Fig. 6C–F and Supplementary Fig. 4) suggests that irradiation increases the relative cellular DNMT activity. Lower nuclear expression of DNMT1 was associated with higher levels in the cytoplasm (Fig. 6E and F). Collectively, these results show that irradiation remodels the enzymatic activity and subcellular localization of DNMT1, suggesting a role in irradiation-induced DNA methylation changes.

Interestingly, 1,685 DMRs overlapped between adipocytes and satellite cells from irradiated mice. The direction of methylation change (i.e., hypo- or hypermethylation) among cell types was similar for 870 DMRs representing genes involved in metabolic processes, chromatin modification, and cell cycle processes (Supplementary Fig. 6). We found a significant interaction between HFD and exposure to ionizing radiation on DNA methylation of 810 genes in adipocytes and 965 genes in satellite cells. Of these genes, only 33 were altered in both cell types, suggesting interaction of HFD and exposure to ionizing radiation manifests in a cell-specific manner. Collectively, these results indicate that ionizing radiation induces coordinated long-term change

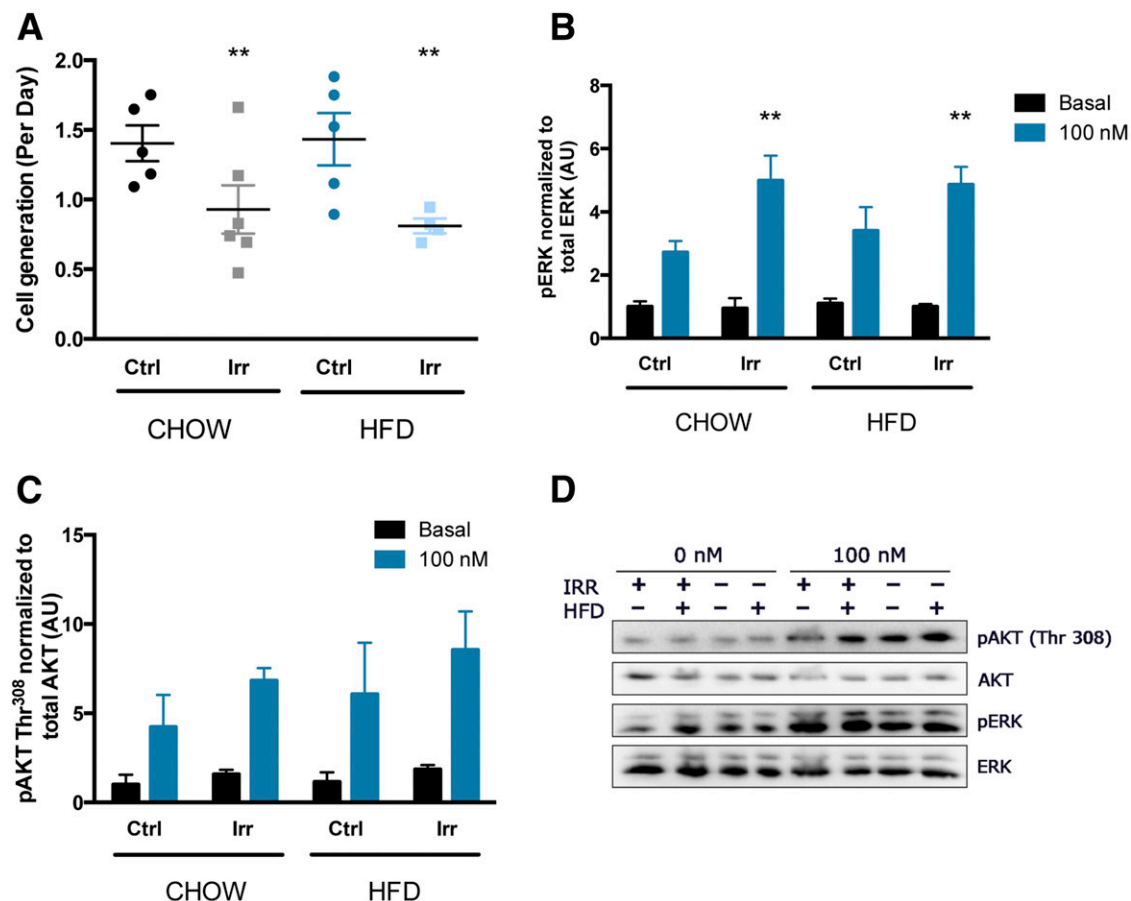


**Figure 4**—Irradiation alters insulin-stimulated ERK signaling of skeletal muscle progenitor cells. Satellite cells were isolated from irradiated (6 Gy) and nonirradiated mice and grown in vitro to test for long-term memory of irradiation ( $N = 6$ ). **A**: Cell proliferation of satellite cells. On day 6 of differentiation cells were stimulated with 0 or 100 nmol/L insulin for 5 min. Phosphorylation of ERK (**B**) and AKT (**C**) was determined by Western blot. Data are presented as fold change compared with Ctrl chow basal. **D**: Representative blots. Error bars are SEM.  $^{**}P < 0.05$  for irradiation only. AU, arbitrary units; Ctrl, nonirradiated; Irr, irradiated.

in gene expression and DNA methylation, which could contribute to the reprogramming of skeletal muscle progenitor cells.

To investigate if DNA methylation changes are linked to gene expression, RNA sequencing was performed on isolated skeletal muscle progenitor cells. We found 827 genes differentially expressed in skeletal muscle cells from irradiated mice compared with cells from nonirradiated mice ( $P < 0.05$ ; FDR  $< 0.05$ ) (Supplementary Table 4), of which 377 genes were downregulated and 450 upregulated. Gene ontology analysis of the differentially expressed genes showed that pathways regulating cellular development, cell death, and oxidative phosphorylation were enriched. Among the differentially expressed genes, 221 genes were both differentially expressed and methylated. For the majority (65%) of these genes, mRNA expression was negatively associated with DNA methylation (Supplementary Table 5). Gene ontology analysis showed that the genes showing inverse correlation between methylation and expression are involved in developmental processes and apoptotic processes (Supplementary Fig. 5), such as axin2 [involved

in WNT signaling (36)], caspase 3 (37), and protein kinase C $\delta$  (log fold change 0.95) (38). Genes belonging to the insulin-signaling pathway like the p85 regulatory subunit of the phosphoinositide 3-kinase, genes involved in the response to oxidative stress like glutathione peroxidase 4 (39), and genes involved in cell proliferation like Cdkn1b (or p27) were also differentially expressed and methylated (40). Collectively, our results indicate that irradiation reprograms the epigenome of skeletal muscle progenitor cells and provides a mechanism by which irradiation could impair cell differentiation and metabolism.

#### Irradiation of Isolated Muscle Cells Recapitulates Ex Vivo Effects

To investigate if the reprogramming of skeletal muscle progenitor cells is caused by a direct effect of ionizing radiation on the muscle cell, L6 rat myoblast cells were irradiated with 0, 1, 3, or 6 Gy of X-ray. Four weeks after irradiation, skeletal muscle cells differentiated into myotubes showed unchanged insulin-stimulated AKT phosphorylation, whereas ERK phosphorylation was potentiated in irradiated

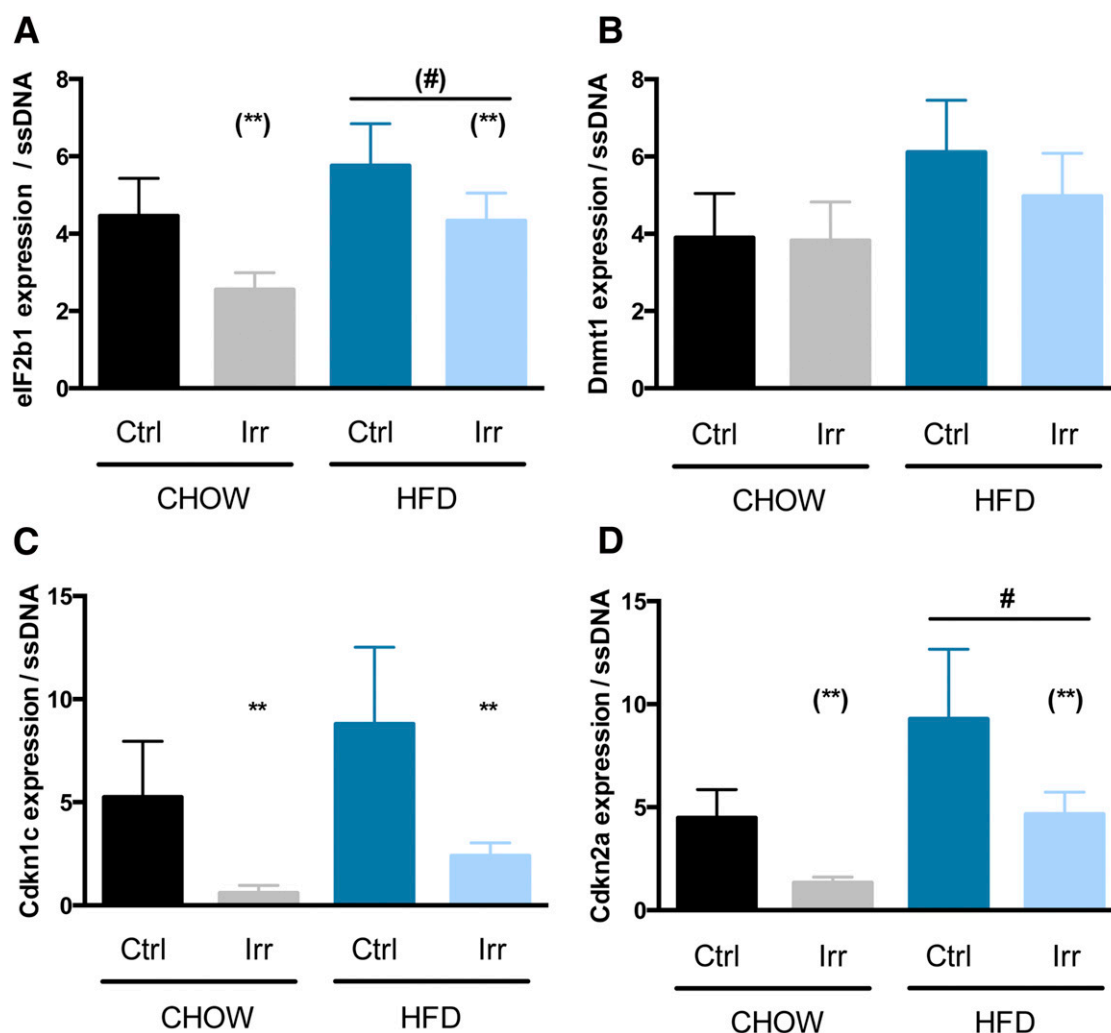


**Figure 5**—Gene expression is changed in muscle progenitor cells irradiated in vivo. mRNA expression of genes located the nearest to the DMRs identified in MBD-Seq was determined by qRT-PCR. Results are relative to ssDNA ( $N = 6$ ). A: eIF2b1. B: Dnmt1. C: Cdkn1c. D: Cdkn2a. Error bars are SEM. \*\* $P < 0.05$  for irradiation only; # $P < 0.05$  for HFD only. Parentheses highlight statistical trend. Ctrl, non-irradiated; Irr, irradiated.

cells (Fig. 7A and B). These results suggest that ionizing radiation alone (and not circulating or neuronal factors, for example) reprograms muscle progenitor cells.

The proliferative capacity and differentiation potential of cells previously exposed to ionizing radiation was determined. Cell proliferation was unaffected at either 1 day or 1 week after exposure to a dose of 2 Gy regardless of cotreatment with antioxidants or folic acid (Supplementary Fig. 7). Using an immunofluorescence assay, we found 80% more myogenin-expressing cells at a late stage of differentiation in cultures previously exposed to ionizing radiation (Fig. 7D), indicating that ionizing radiation of in vitro skeletal muscle cell cultures does not change proliferation but impairs differentiation potential.

## DISCUSSION

In this study, we report that ionizing radiation increases the risk for insulin resistance in mice fed an HFD and

disturbs growth homeostasis of fat and skeletal muscle in mice fed an HFD. Using ex vivo cultures of skeletal muscle and fat progenitor cells, we show that exposure to ionizing radiation reprograms the epigenome of these cells, specifically at genes controlling the cell cycle, metabolism, and epigenetic modifiers. Thus, epigenetic changes in peripheral tissues controlling glucose homeostasis and body mass may influence the risk for metabolic disease after cancer treatment.

Irradiation (6 Gy) was associated with lower total body weight in mice throughout life, with changes in lean and fat mass accounting for the difference. Interestingly, irradiated mice fed a chow diet had greater insulin sensitivity. This is consistent with the well-documented observation that reduced adiposity is associated with increased insulin sensitivity (41). However, irradiated mice fed an HFD (60%) showed lower fat mass and insulin sensitivity compared with control mice. This could



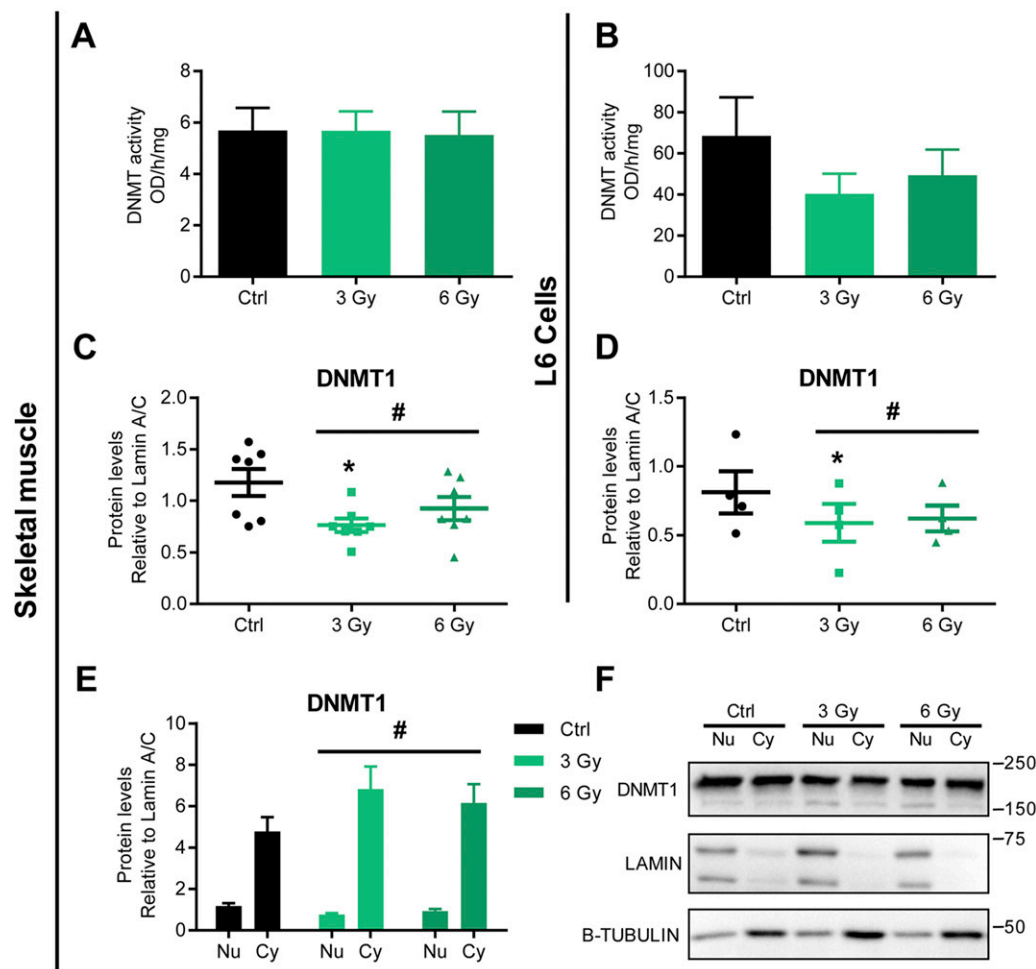


**Figure 6**—Irradiation regulates DNMT1 expression and subcellular localization in skeletal muscle. Eight-week-old C57Bl/6 mice ( $N = 7$ ) and L6 cells ( $N = 4$ ) were exposed to a 3- or 6-Gy irradiation or sham treated. At 24 h postirradiation, total DNMT activity was investigated in gastrocnemius skeletal muscle (A) and L6 cells (B). DNMT1 protein expression was measured in gastrocnemius (C) and L6 cells (D). Subcellular localization of DNMT1 was assessed in gastrocnemius skeletal muscle (E and F). Representative Western blot images are presented (F). Error bars are SEM. \* $P < 0.05$ ; # highlights  $P < 0.05$  interaction between group and localization. Ctrl, nonirradiated; Cy, cytoplasm; Nu, nucleus; OD, optical density.

be due to a lack of adipose tissue plasticity and consequent lipodystrophy after ionizing radiation (42). Although lipodystrophy is associated with ectopic fat deposition, notably in metabolic organs, crude examinations of the animal postmortem did not reveal an exacerbated liver steatosis in irradiated mice compared with nonirradiated control.

In this study, we show that ionizing radiation potentiates insulin-stimulated ERK signaling. Given that ERK signaling and alteration in the balance between insulin-responsive ERK and AKT signaling are associated with decreased insulin signaling (35), radiation-induced potentiation of ERK signaling, which occurred in both skeletal muscle and fat progenitors, could be a mechanism by which ionizing radiation induces peripheral insulin resistance.

Ionizing radiation remodels the epigenome of skeletal muscle and fat progenitor cells. Although total nucleus activity of DNMTs was not changed 24 h after irradiation, our observation that DNMT1 expression levels and

subcellular compartmentalization were altered after ionizing radiation implies that relative DNMT1 enzymatic activity is changed after irradiation. Other studies showed that compartmentalization of deacetylase Sirtuin 1 occurs acutely in response to DNA damage, which mediates silencing of damaged genes during DNA repair (43). Thus, we propose that ionizing radiation, potentially through DNA damage, induces epigenetic remodeling through the regulation of epigenetic modifiers.

Our epigenomic and transcriptomic analyses revealed that changes in DNA methylation are not always associated with changes in gene expression. Such discrepancy is in accordance with a study showing as little as 25% of DMRs inversely correlate with gene expression changes (44). We can only speculate that DNA methylation changes remain nonfunctional until a secondary physiological or environmental stress activates specific transcription factors and that the binding capability of such transcription factors

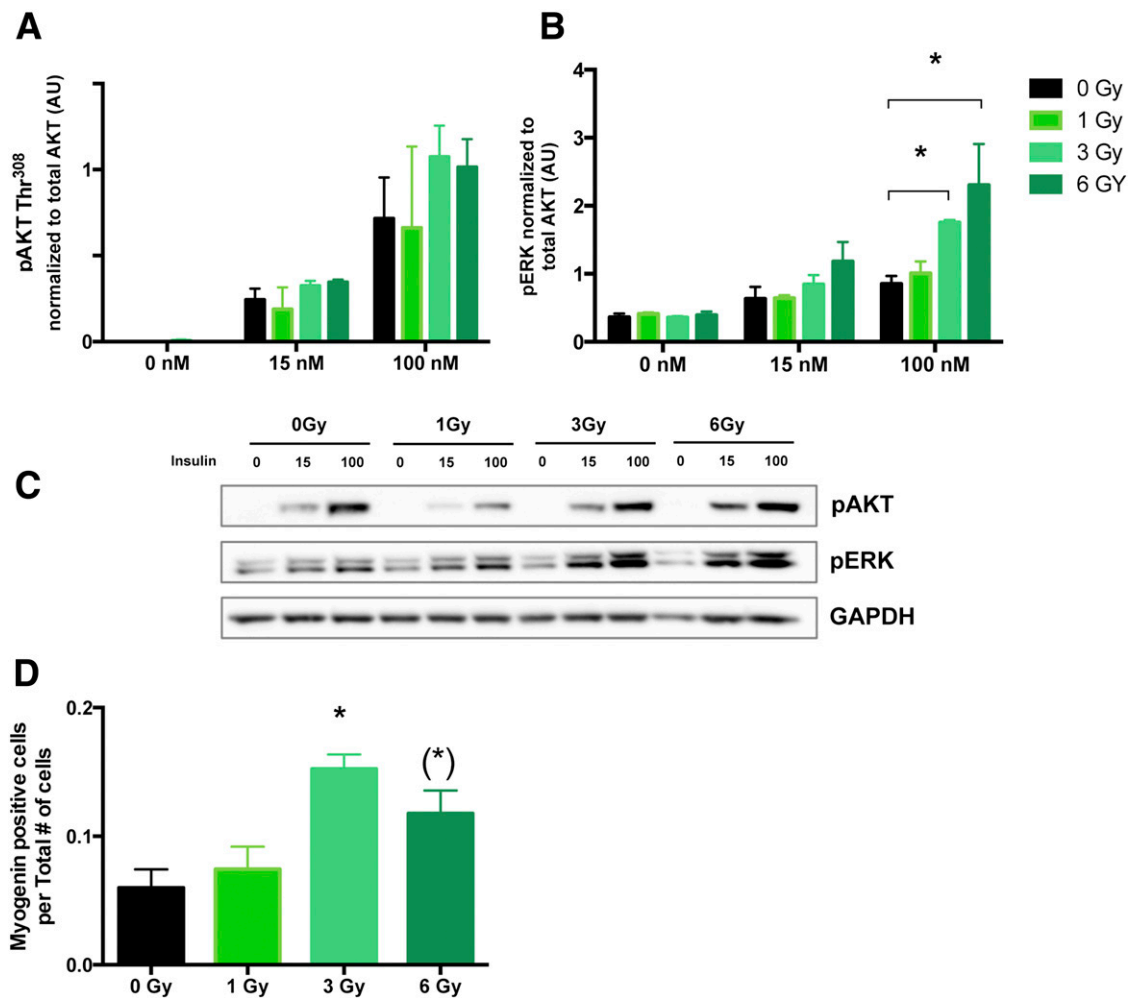


**Figure 7**—Insulin-induced phosphorylation of ERK is potentiated in myoblast cell lines. Rat myoblasts were irradiated with 1, 3, or 6 Gy of X-ray ( $N = 3$ ), and nonirradiated control were sham treated ( $N = 3$ ). After 4 weeks of recovery, myocytes were differentiated into myotubes. On day 8 of differentiation, myotubes were stimulated with 0, 15, or 100 nmol/L insulin for 5 min. Phosphorylation of ERK and AKT was determined by Western blot. **A**: AKT phosphorylation. **B**: ERK phosphorylation. **C**: Representative blot showing phosphorylation of ERK, phosphorylation of AKT, and GAPDH (loading control). **D**: Myogenin expression was quantified by immunofluorescence. Data are presented as ratio of myogenin-expressing cells relative to total cell count. Error bars are SEM.  $*P < 0.05$ . Parentheses highlight statistical trend. AU, arbitrary units.

will be altered due to the DMRs. For instance, such priming occurs in pregnancy in which the mammary gland undergoes substantial chronic epigenetic remodeling that only causes an effect during lactation when relevant transcription factors are expressed (45). However, a major proportion (65%) of genes both differentially methylated and expressed showed an inverse association between gene expression and DNA methylation in skeletal muscle progenitor cells. The fact that these genes are associated with ontology terms including apoptosis and developmental processes support the notion that epigenetic remodeling drives the immediate phenotype we observed on disturbed proliferation, differentiation, and ERK-stimulated insulin pathway.

We found that *Cdkn1* expression and methylation were changed concomitantly to greater ERK signaling in satellite cells exposed to irradiation. Both factors are mostly mitogenic (46); however, this contrasts with the finding

of lower satellite cell proliferation capacity and suggests that decreased *Cdkn* expression mediates other effects. The downstream effects of *Cdkn* signaling are highly context dependent, as exemplified by the action of *Cdkn1a*, which inhibits or induces apoptosis depending on its intracellular localization (47). Additionally, *Cdkn1c* can contribute to terminal skeletal muscle differentiation through the modulation of myogenic differentiation (*MyoD*) expression (48). Moreover, aged satellite cells are characterized both by increased proliferation rate and increased apoptosis rate, but the net result is a decreased cell number (49). Thus, ionizing radiation likely disrupts the balance between proliferation and apoptosis.

Bystander effects constitute a phenomenon by which nonirradiated cells exhibit an identical phenotype as compared with the directly irradiated cells (50). To determine if ionizing radiation affected the skeletal muscle cells directly

or by a bystander effect, we compared proliferation and intracellular signaling pathways of skeletal muscle cells irradiated in vivo or in culture. Because similar effects were found in both models, our results suggest that irradiation affects skeletal muscle progenitor cell through a predominant direct, nonbystander effect.

In conclusion, our results provide insight into mechanisms by which ionizing radiation affects skeletal muscle and adipose progenitor cells. We show that ionizing radiation alters epigenetic modifiers, remodels the epigenome of progenitor cells, and impairs capacity to differentiate. Epigenetic factors may be involved in the long-term side effects of radiation, notably on metabolic health when used in cancer therapy.

**Acknowledgments.** The authors thank Steve Risis, Novo Nordisk Foundation Center for Basic Metabolic Research, University of Copenhagen, for assistance with the mice experiments; Sara Gry Vienberg, Novo Nordisk Foundation Center for Basic Metabolic Research, University of Copenhagen, for assistance with the SVF isolations and mice experiments; and Anne Grapin-Botton and Gelo Dela Cruz, DanStem, University of Copenhagen, for assistance with cell sorting.

**Funding.** This work was supported by the European Foundation for the Study of Diabetes (EFSD Research Programme in Diabetes and Cancer). The Novo Nordisk Foundation Center for Basic Metabolic Research is an independent Research Center at the University of Copenhagen partially funded by an unrestricted donation from the Novo Nordisk Foundation (<http://www.metabol.ku.dk>). O.F. received a fellowship from the Danish Diabetes Academy.

**Duality of Interest.** No potential conflicts of interest relevant to this article were reported.

**Author Contributions.** V.N., E.A., O.F., M.R., K.C., G.L.C., and M.A. contributed to data acquisition. V.N., L.R.I., E.A., O.F., C.G., D.S., and R.B. contributed to data analysis. V.N., M.A., L.S., D.S., and R.B. contributed to the study design. V.N., L.R.I., E.A., O.F., C.G., M.R., K.C., J.B., G.L.C., M.A., L.S., D.S., and G.B. contributed to data interpretation and manuscript drafting and approved the final version of the manuscript. D.S. and R.B. were responsible for the integrity of the work as a whole. R.B. is the guarantor of this work and, as such, had full access to all the data in the study and takes responsibility for the integrity of the data and the accuracy of the data analysis.

## References

- Preston DL, Shimizu Y, Pierce DA, Suyama A, Mabuchi K. Studies of mortality of atomic bomb survivors. Report 13: Solid cancer and noncancer disease mortality: 1950–1997. *Radiat Res* 2003;160:381–407
- Yamada M, Wong FL, Fujiwara S, Akahoshi M, Suzuki G. Noncancer disease incidence in atomic bomb survivors, 1958–1998. *Radiat Res* 2004;161:622–632
- Oudin C, Simeoni MC, Sirvent N, et al. Prevalence and risk factors of the metabolic syndrome in adult survivors of childhood leukemia. *Blood* 2011;117:4442–4448
- Neville KA, Cohn RJ, Steinbeck KS, Johnston K, Walker JL. Hyperinsulinemia, impaired glucose tolerance, and diabetes mellitus in survivors of childhood cancer: prevalence and risk factors. *J Clin Endocrinol Metab* 2006;91:4401–4407
- Baker KS, Ness KK, Steinberger J, et al. Diabetes, hypertension, and cardiovascular events in survivors of hematopoietic cell transplantation: a report from the bone marrow transplantation survivor study. *Blood* 2007;109:1765–1772
- Meacham LR, Sklar CA, Li S, et al. Diabetes mellitus in long-term survivors of childhood cancer. Increased risk associated with radiation therapy: a report for the childhood cancer survivor study. *Arch Intern Med* 2009;169:1381–1388
- Thompson LH, Suit HD. Proliferation kinetics of x-irradiated mouse L cells studied with time-lapse photography. I. Experimental methods and data analysis. *Int J Radiat Biol Relat Stud Phys Chem Med* 1967;13:391–397
- Latella L, Lukas J, Simone C, Puri PL, Bartek J. Differentiation-induced radioresistance in muscle cells. *Mol Cell Biol* 2004;24:6350–6361
- DeFronzo RA, Gunnarsson R, Björkman O, Olsson M, Wahren J. Effects of insulin on peripheral and splanchnic glucose metabolism in noninsulin-dependent (type II) diabetes mellitus. *J Clin Invest* 1985;76:149–155
- Abel ED, Peroni O, Kim JK, et al. Adipose-selective targeting of the GLUT4 gene impairs insulin action in muscle and liver. *Nature* 2001;409:729–733
- Meissner A. Epigenetic modifications in pluripotent and differentiated cells. *Nat Biotechnol* 2010;28:1079–1088
- Kuhmann C, Weichenhan D, Rehli M, Plass C, Schmezer P, Popanda O. DNA methylation changes in cells regrowing after fractionated ionizing radiation. *Radiother Oncol* 2011;101:116–121
- Raiche J, Rodriguez-Juarez R, Pogribny I, Kovalchuk O. Sex- and tissue-specific expression of maintenance and de novo DNA methyltransferases upon low dose X-irradiation in mice. *Biochem Biophys Res Commun* 2004;325:39–47
- Weitzman SA, Turk PW, Milkowski DH, Kozlowski K. Free radical adducts induce alterations in DNA cytosine methylation. *Proc Natl Acad Sci U S A* 1994;91:1261–1264
- Kaup S, Grandjean V, Mukherjee R, et al. Radiation-induced genomic instability is associated with DNA methylation changes in cultured human keratinocytes. *Mutat Res* 2006;597:87–97
- Montarras D, Morgan J, Collins C, et al. Direct isolation of satellite cells for skeletal muscle regeneration. *Science* 2005;309:2064–2067
- Mackey AL, Kjaer M, Charifi N, et al. Assessment of satellite cell number and activity status in human skeletal muscle biopsies. *Muscle Nerve* 2009;40:455–465
- Tedesco FS, Dellavalle A, Diaz-Manera J, Messina G, Cossu G. Repairing skeletal muscle: regenerative potential of skeletal muscle stem cells. *J Clin Invest* 2010;120:11–19
- Cerletti M, Jurka S, Witczak CA, et al. Highly efficient, functional engraftment of skeletal muscle stem cells in dystrophic muscles. *Cell* 2008;134:37–47
- Christensen GL, Jacobsen ML, Wendt A, et al. Bone morphogenetic protein 4 inhibits insulin secretion from rodent beta cells through regulation of calbindin1 expression and reduced voltage-dependent calcium currents. *Diabetologia* 2015;58:1282–1290
- Barrès R, Yan J, Egan B, et al. Acute exercise remodels promoter methylation in human skeletal muscle. *Cell Metab* 2012;15:405–411
- Donkin I, Versteyhe S, Ingerslev LR, et al. Obesity and Bariatric Surgery Drive Epigenetic Variation of Spermatozoa in Humans. *Cell Metab* 2016;23:369–378
- Bolger AM, Lohse M, Usadel B. Trimmomatic: a flexible trimmer for Illumina sequence data. *Bioinformatics* 2014;30:2114–2120
- Langmead B, Salzberg SL. Fast gapped-read alignment with Bowtie 2. *Nat Methods* 2012;9:357–359
- Liao Y, Smyth GK, Shi W. The Subread aligner: fast, accurate and scalable read mapping by seed-and-vote. *Nucleic Acids Res* 2013;41:e108
- Robinson MD, McCarthy DJ, Smyth GK. edgeR: a Bioconductor package for differential expression analysis of digital gene expression data. *Bioinformatics* 2010;26:139–140
- Krueger F, Andrews SR. Bismark: a flexible aligner and methylation caller for Bisulfite-Seq applications. *Bioinformatics* 2011;27:1571–1572
- Hebestreit K, Dugas M, Klein HU. Detection of significantly differentially methylated regions in targeted bisulfite sequencing data. *Bioinformatics* 2013;29:1647–1653
- Kim D, Pertea G, Trapnell C, Pimentel H, Kelley R, Salzberg SL. TopHat2: accurate alignment of transcriptomes in the presence of insertions, deletions and gene fusions. *Genome Biol* 2013;14:R36
- Liao Y, Smyth GK, Shi W. featureCounts: an efficient general purpose program for assigning sequence reads to genomic features. *Bioinformatics* 2014;30:923–930
- Huang MB, Xu H, Xie SJ, Zhou H, Qu LH. Insulin-like growth factor-1 receptor is regulated by microRNA-133 during skeletal myogenesis. *PLoS One* 2011;6:e29173

32. Eden E, Navon R, Steinfeld I, Lipson D, Yakhini Z. GOrilla: a tool for discovery and visualization of enriched GO terms in ranked gene lists. *BMC Bioinformatics* 2009;10:48
33. Harman-Boehm I, Blüher M, Redel H, et al. Macrophage infiltration into omental versus subcutaneous fat across different populations: effect of regional adiposity and the comorbidities of obesity. *J Clin Endocrinol Metab* 2007;92:2240–2247
34. Xu H, Barnes GT, Yang Q, et al. Chronic inflammation in fat plays a crucial role in the development of obesity-related insulin resistance. *J Clin Invest* 2003;112:1821–1830
35. Yu X, Shen N, Zhang ML, et al. Egr-1 decreases adipocyte insulin sensitivity by tilting PI3K/Akt and MAPK signal balance in mice. *EMBO J* 2011;30:3754–3765
36. Figeac N, Zammit PS. Coordinated action of Axin1 and Axin2 suppresses  $\beta$ -catenin to regulate muscle stem cell function. *Cell Signal* 2015;27:1652–1665
37. Porter AG, Jänicke RU. Emerging roles of caspase-3 in apoptosis. *Cell Death Differ* 1999;6:99–104
38. Jackson DN, Foster DA. The enigmatic protein kinase Cdelta: complex roles in cell proliferation and survival. *FASEB J* 2004;18:627–636
39. Ran Q, Liang H, Gu M, et al. Transgenic mice overexpressing glutathione peroxidase 4 are protected against oxidative stress-induced apoptosis. *J Biol Chem* 2004;279:55137–55146
40. Hipfner DR, Cohen SM. Connecting proliferation and apoptosis in development and disease. *Nat Rev Mol Cell Biol* 2004;5:805–815
41. Kahn SE, Hull RL, Utzschneider KM. Mechanisms linking obesity to insulin resistance and type 2 diabetes. *Nature* 2006;444:840–846
42. Petersen KF, Shulman GI. Etiology of insulin resistance. *Am J Med* 2006;119(Suppl. 1):S10–S16
43. Oberdoerffer P, Michan S, McVay M, et al. SIRT1 redistribution on chromatin promotes genomic stability but alters gene expression during aging. *Cell* 2008;135:907–918
44. Rönn T, Volkov P, Davegårdh C, et al. A six months exercise intervention influences the genome-wide DNA methylation pattern in human adipose tissue. *PLoS Genet* 2013;9:e1003572
45. Dos Santos CO, Dolzhenko E, Hodges E, Smith AD, Hannon GJ. An epigenetic memory of pregnancy in the mouse mammary gland. *Cell Reports* 2015;11:1102–1109
46. Worster DT, Schmelzle T, Solimini NL, et al. Akt and ERK control the proliferative response of mammary epithelial cells to the growth factors IGF-1 and EGF through the cell cycle inhibitor p57Kip2. *Sci Signal* 2012;5:ra19
47. Cazzalini O, Scovassi AI, Savio M, Stivala LA, Prosperi E. Multiple roles of the cell cycle inhibitor p21(CDKN1A) in the DNA damage response. *Mutat Res* 2010;704:12–20
48. Osborn DP, Li K, Hinits Y, Hughes SM. Cdkn1c drives muscle differentiation through a positive feedback loop with MyoD. *Dev Biol* 2011;350:464–475
49. Chakkalakal JV, Jones KM, Basson MA, Brack AS. The aged niche disrupts muscle stem cell quiescence. *Nature* 2012;490:355–360
50. Mothersill C, Seymour C. Radiation-induced bystander effects: past history and future directions. *Radiat Res* 2001;155:759–767